

Constraining Halo Occupation Distribution and Cosmic Growth Rate using Multipole Power Spectrum

Chiaki Hikage¹

¹ *Kobayashi-Maskawa Institute for the Origin of Particles and the Universe (KMI), Nagoya University, 464-8602, Japan*

3 December 2024

ABSTRACT

We propose a new method of measuring halo occupation distribution (HOD) together with cosmic growth rate using multipole components of galaxy power spectrum $P_l(k)$. The non-linear redshift-space distortion due to the random motion of satellite galaxies, i.e., Fingers-of-God, generates high- l multipole anisotropy in galaxy clustering such as the hexadecapole ($l = 4$) and tetra-hexadecapole ($l = 6$), which are sensitive to the fraction and the velocity dispersion of satellite galaxies. Using simulated samples following the HOD of Luminous Red Galaxies (LRG), we find that the input HOD is successfully reproduced using $P_l(k)$ even when directly fitting the central and satellite HOD values at different bins of mass without assuming any functional form. We also show that the measurements of the cosmic growth rate as well as the satellite fraction and velocity dispersions are significantly improved by adding the small-scale information of high- l multipoles.

Key words: cosmology: theory – observations – large-scale structure of the Universe – galaxies: kinematics and dynamics

1 INTRODUCTION

Understanding the relationship between galaxy distributions and their host dark matter halos is a key ingredient in the physics of galaxy formation and is also important for precision cosmology study using galaxy datasets. Halo occupation distribution (HOD) describes the probability distribution of the occupation number of central and satellite galaxies as a function of their host halo mass (e.g., Berlind & Weinberg 2002; Berlind et al. 2003; Kravtsov et al. 2004; Zheng et al. 2005). Abundance matching of simulated subhalos to connect the properties of galaxies has been widely investigated (e.g., Masaki et al. 2013). HOD has been measured from a variety of galaxy samples using projected correlation function which is sensitive to the radial profile of galaxies (e.g., Zehavi et al. 2005; Masjedi et al. 2006; Zheng et al. 2009; White et al. 2011; Geach et al. 2012). Multiplicity functions using some group-finding technique has been also used to study the relation of the host halo with the properties of galaxies and also satellite kinematics (e.g., Reid & Spergel 2009). Cross correlation of galaxies with background galaxy image distortions, i.e., galaxy-galaxy lensing, has been measured to connect the halo mass with the galaxy properties (e.g., Mandelbaum et al. 2006). The dilution of the lensing signal around off-centered (satellite) galaxies provides a probe of the satellite fraction and the velocity dispersion (Hikage et al. 2012; George et al. 2012; Hikage et al. 2013).

We propose a novel method to constrain HOD using the multipole galaxy power spectra $P_l(k)$ by characterizing the anisotropy of the galaxy clustering due to the redshift-space distortion (RSD). The random motion of galaxies inside their host halos generates

the nonlinear redshift-space distortion, i.e., Fingers-of-God (FoG) effect (Jackson 1972). As the off-centered or satellite galaxies have large internal motion, the FoG effect provides a useful probe of constraining the fraction of satellite galaxies. Hikage & Yamamoto (2013) recently clearly detect high- l multipole anisotropy such as hexadecapole ($l = 4$) and tetra-hexadecapole ($l = 6$) due to the satellite FoG effect. In the framework of halo model, the signature comes from the FoG effect of one-halo term, the contributions of central-satellite and satellite-satellite pair hosted by the same halos.

In this letter, we utilize such high- l multipole anisotropy to constrain HOD. Focused on the luminous red galaxies (LRG), which has been widely used for cosmology analysis in SDSS (Eisenstein et al. 2001), we construct simulated mock samples of LRGs on the HOD basis. We show that the input HOD is reproduced even when fitting $P_l(k)$ with central and satellite HODs at different bins of mass without assuming any functional form. High- l multipole is sensitive to satellite velocity distribution, while the projected correlation function depends on the radial profile of satellite galaxies in the host halos. Both measurements play complementary roles in understanding the relationship between galaxies and halos.

The bulk motion of galaxies drives the anisotropy in galaxy clustering, which provides a powerful observational probe of measuring the cosmic growth rate to test General Relativity and various gravity models (Peacock et al. 2001; Okumura et al. 2008; Guzzo et al. 2008). Combinations of monopole ($l = 0$) and quadrupole ($l = 2$) power spectra has been widely used to constrain growth rate from various galaxy samples including SDSS LRG (Yamamoto et al. 2008, 2010; Sato et al. 2011; Oka et al. 2013) and recently

BOSS CMASS sample (Reid et al. 2012; Beutler et al. 2013; Samushia et al. 2013). Satellite FoG effect is a major systematic uncertainty in measuring the growth rate in this analysis. Even when the satellite fraction of the SDSS LRG sample is just 6%, the measurement of growth rate can be strongly biased (Hikage & Yamamoto 2013). As high- l multipole spectra such as P_4 and P_6 are sensitive to the satellite fraction, they are useful for eliminating the uncertainty of the satellite FoG. Using the simulated halo power spectra directly, we show that the measurement of growth rate is significantly improved by adding high- l multipole information.

This letter is organized as follows: in section 2, we present the theoretical formalism to describe the multipole power spectra based on the halo model. In section 3, we summarize how to make simulation data for LRG catalogs. The results of the measurements of HOD, and the growth rate from P_l are summarized in section 4. Section 5 is devoted to summary and conclusions. Throughout the letter, we use flat Λ CDM model and fix cosmological parameters as follows: $\Omega_b h^2 = 0.0226$, $\Omega_c h^2 = 0.1108$, $n_s = 0.963$, $h = 0.704$, $\tau = 0.089$, $\sigma_8 = 0.817$.

2 FORMALISM

In this section, we summarize our theoretical formulae of the multipole power spectra based on halo model. We focus on the luminous red galaxy (LRG) and present how to parametrize their HOD.

2.1 Multipole power spectra in halo model

Galaxy power spectrum in redshift space $P(k, \mu)$, where μ is the line-of-sight component with respect to the absolute value of the wavevector k , is described by expanding their multipole components:

$$P_l(k) = \frac{2l+1}{2} \int_{-1}^1 d\mu P(k, \mu) \mathcal{L}_l(\mu), \quad (1)$$

where \mathcal{L}_l is l -th Legendre polynomials. In the halo-model approach (e.g., Seljak 2000; White 2001; Cooray & Sheth 2002), the galaxy power spectrum can be decomposed into the 1-halo and 2-halo terms,

$$P(k, \mu) = P^{1h}(k, \mu) + P^{2h}(k, \mu). \quad (2)$$

One-halo term is the contribution from the clustering of central-satellite and satellite-satellite pairs hosted by same halos and written as follows:

$$P^{1h}(k, \mu) = \frac{1}{n_{\text{tot}}^2} \int dM \frac{dn_h}{dM} \left[2 \langle N_{\text{cen}} \rangle \langle N_{\text{sat}} \rangle \tilde{p}_{\text{sat}}(k, \mu; M) + \langle N_{\text{sat}} (N_{\text{sat}} - 1) \rangle \tilde{p}_{\text{sat}}^2(k, \mu; M) \right], \quad (3)$$

where dn_h/dM is the halo mass function, $\langle N_{\text{cen}} \rangle$ and $\langle N_{\text{sat}} \rangle$ denote the HOD of central and satellite galaxies respectively, n_{tot} is the total number density of galaxies (see the details of HOD parametrization in the next subsection). We assume that the occupation number of satellite galaxies follows Poisson statistics, which implies $\langle N_{\text{sat}} (N_{\text{sat}} - 1) \rangle = \langle N_{\text{cen}} \rangle \langle N_{\text{sat}} \rangle^2$ (Kravtsov et al. 2004; Zehavi et al. 2005). Here we assume that the halo hosting satellite LRGs must have a central LRG. This assumption is good for our purpose, though some of central galaxies are not always LRG (e.g., Skibba et al. 2011). The satellite distribution around central galaxies inside the halo with mass M is described with $\tilde{p}_{\text{sat}}(k, \mu; M)$.

We neglect the velocity dispersion of central galaxies. The distribution of satellite galaxies in their host halo follows dark matter distribution and the radial profile of satellite galaxies follows the NFW profile (Navarro et al. 1997) with the concentration given by Duffy et al. (2008). The internal velocity of satellite galaxies has Gaussian distribution with the velocity dispersion determined by their host halo mass:

$$\tilde{p}_{\text{sat}}(k, \mu, M) = \tilde{u}_{\text{NFW}}(k; M) \exp \left[-\frac{\sigma_v^{(\text{vir})2}(M) k^2 \mu^2}{2a^2 H^2(z)} \right], \quad (4)$$

where the velocity dispersion of satellite galaxies is given by the Virial velocity dispersion $\sigma_v^{(\text{vir})} \equiv (GM/2r_{\text{vir}})^{1/2}$ and $\tilde{u}_{\text{NFW}}(k)$ is the Fourier transform of the NFW density profile. The average velocity dispersion of satellite galaxies become

$$\sigma_v^{(\text{sat})} = \left[\frac{1}{n_{\text{sat}}} \int dM \frac{dn_h}{dM} \langle N_{\text{cen}} \rangle \langle N_{\text{sat}} \rangle \sigma_v^{(\text{vir})2} \right]^{1/2}, \quad (5)$$

where n_{sat} is the number density of satellite galaxies. The satellite fraction f_{sat} is defined as $n_{\text{sat}}/n_{\text{tot}}$.

The two-halo term, which is the contribution of the clustering of LRGs in different halos, depends on the redshift-space halo power spectra with different halo masses $P_{\text{hh}}(k; M, M')$ (Hikage et al. 2013):

$$P^{2h}(k, \mu) = \frac{1}{n_{\text{tot}}^2} \int dM \frac{dn_h}{dM} \int dM' \frac{dn_h}{dM'} \times [\langle N_{\text{cen}} \rangle (1 + \langle N_{\text{sat}} \rangle \tilde{p}_{\text{sat}}(k, \mu; M))] \times [\langle N_{\text{cen}} \rangle (1 + \langle N_{\text{sat}} \rangle \tilde{p}_{\text{sat}}(k, \mu; M'))] P_{\text{hh}}(k, \mu; M, M'). \quad (6)$$

The 2-halo term is affected by FoG effect through the distribution function of satellite galaxies in redshift space \tilde{p}_{sat} (eq.[4]) while the central galaxy locates on the center of the host halo and the internal motion is negligible. We directly estimate the redshift-space halo power spectra $P_{\text{hh}}(k, \mu; M, M')$ using simulations because they involve various nonlinear effects due to the gravitational evolution, the halo biasing, and the motion of halos. We divide the simulated halo samples into 10 different mass bins to compute their auto- and cross-halo power spectra in redshift space (see section 3 for details).

2.2 Parametrization of Halo Occupation Distribution (HOD)

We consider two different ways to describe HOD of central and satellite LRGs.

(i) One is using a following functional form of HOD (Zheng et al. 2005):

$$\langle N_{\text{cen}} \rangle = \frac{1}{2} \left[1 + \text{erf} \left(\frac{\log_{10}(M) - \log_{10}(M_{\text{min}})}{\sigma_{\log M}} \right) \right], \quad (7)$$

$$\langle N_{\text{sat}} \rangle = \left(\frac{M - M_{\text{cut}}}{M_1} \right)^\alpha, \quad (8)$$

where $\text{erf}(x)$ is the error function and five HOD parameters are included. The fiducial values of the HOD parameters for SDSS DR7 LRG sample is set as $M_{\text{min}} = 5.7 \times 10^{13} h^{-1} M_\odot$, $\sigma_{\log M} = 0.7$, $M_{\text{cut}} = 3.5 \times 10^{13} h^{-1} M_\odot$, $M_1 = 3.5 \times 10^{14} h^{-1} M_\odot$, and $\alpha = 1$ (Reid & Spergel 2009).

(ii) The other way is not assuming any functional form of HOD. We parametrize central and satellite HODs at different mass and interpolate the HOD of intermediate halo mass in spline approximation. We divide 5 different mass bins (10 HOD parameters in

total) in the mass range from $10^{12} h^{-1} M_{\odot}$ to $10^{15} h^{-1} M_{\odot}$. We assume that the satellite number $\langle N_{\text{sat}} \rangle$ monotonically increases as halo mass M is larger.

3 SIMULATION DATA WITH THE HOD OF LUMINOUS RED GALAXIES

We construct simulated samples with the HOD of Luminous Red Galaxies (LRG) to estimate the error of HOD parameters and growth rate from the measurements of P_l . We run 100 realizations of N-body simulations using Gadget-2 code (Springel 2005). The initial distribution of mass particles is set using 2LPT code in Gaussian initial condition (Crocce et al. 2006) with the initial redshift of $z = 49$. The initial matter power spectrum is computing using CAMB software (Lewis et al. 2000) with the fiducial cosmological parameters. The N-body simulations are performed in a periodic cubic box at the side length L_{box} of $1 h^{-1} \text{Gpc}$ with the number of mass particles is 800^3 where each particle mass is $1.3 \times 10^{11} h^{-1} M_{\odot}$. Halo is identified by Friends-of-Friends algorithm with the linking length $b = 0.2$. The minimum number of mass particles constituting halos is 20, which corresponds to the halo mass of $2.6 \times 10^{12} h^{-1} M_{\odot}$. The position and velocity of each halo is defined as the arithmetic mean of those of the constituent mass particles of each halo.

We randomly select halos hosting central LRGs and pick up the dark matter particles for satellite LRGs to follow the fiducial HOD (eq. [8]). The number distribution of satellite LRGs follow Poisson statistics. The position and velocity of the host halo and the mass particle are respectively assigned to those of central and satellite LRGs. In the fiducial HOD values, the fraction of satellite galaxies becomes 6.5% and the velocity dispersion of satellites is $\sigma_v^{(\text{sat})} = 570 \text{ km/s}$ in average. For simplicity, the simulations do not include various observational issues such as the angular mask, radial selection function, and fiber collisions.

Number density is assigned to each grid with the nearest grid point (NGP) scheme and the number of grids N_{grid} is set to be 512 at a side. We compute the multipole power spectrum by transforming the density field into Fourier space with Fast Fourier Transform (FFT) method. The shot noise term, the inverse of the number density in the sample, is subtracted from the monopole power spectrum. The covariance of the multipole power spectra P_l at different l and different bins of k is estimated from 100 realizations of simulated samples. We also combine jackknife resampling method and obtain the enough number of realizations to estimate the covariance.

We take z-axis as the line-of-sight direction and obtain the redshift-space position by adding the velocity component v_z

$$s = r + \frac{f_z}{f_z^{(\text{GR})}} \frac{(1+z)v_z}{H(z)}. \quad (9)$$

In order to estimate the deviation of the growth rate f_z from the GR prediction $f_z^{(\text{GR})}$, we simply change the amplitude of velocity by hand (c.f., Nishimichi & Oka 2013).

4 RESULTS

4.1 Satellite FoG effects on multipole power spectra

Figure 1 shows the results of P_4 and P_6 for the simulated samples (black circles) in comparison with the model predictions with the

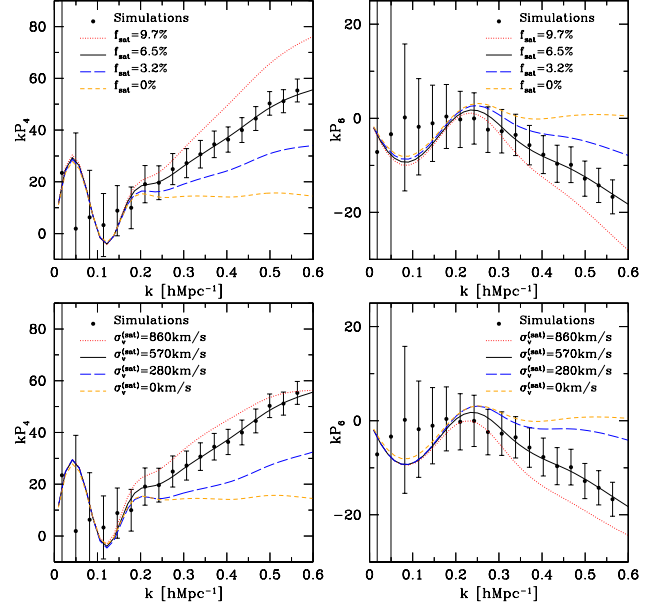


Figure 1. Hexadecapole $P_4(k)$ (left) and tetra-hexadecapole $P_6(k)$ (right) for the mock LRG samples in average (black circles). Error-bars denote the $1\text{-}\sigma$ dispersion. The black lines represent the model prediction with the fiducial values of HOD in which the satellite fraction is $f_{\text{sat}} = 6.5\%$ and the satellite velocity dispersion is $\sigma_v^{(\text{sat})} = 570 \text{ km/s}$. For comparison, we plot the theoretical models by varying f_{sat} (Upper) and $\sigma_v^{(\text{sat})}$ (Lower).

same HOD (black lines). They are found to be in excellent agreement with each other. For comparison, we plot the model predictions by varying satellite fraction f_{sat} and the satellite velocity dispersion $\sigma_v^{(\text{sat})}$. As the 2-halo contribution is small for high- l multipole ($l \geq 4$), they provide good probes of the satellite properties through their velocity distribution or FoG effect. The number of central-satellite and satellite-satellite pairs are proportional to $\langle N_{\text{sat}} \rangle$ and $\langle N_{\text{sat}} \rangle^2$ respectively (see eq.[3]). As the satellite fraction is small for the LRG sample, central-satellite pair contribution is dominant and thus the overall amplitude of P_l ($l \geq 4$) is roughly proportional to f_{sat} . The velocity dispersion of satellites is determined by the typical halo mass hosting satellites. As the velocity dispersion increases, the FoG effect starts at smaller k , while the overall amplitude decreases at large- k limit.

4.2 Reconstructions of HOD from multipole power spectra

We apply Markov Chain Monte Carlo method to the simulated power spectra to estimate the likelihood function of a parameter set \mathbf{p} in the chi-square basis:

$$\chi^2 = \sum_{i,j} [y_i^{(\text{model})}(\mathbf{p}) - y_i^{(\text{sim})}] \text{Cov}_{ij}^{-1} [y_j^{(\text{model})}(\mathbf{p}) - y_j^{(\text{sim})}] + [(N_{\text{tot}}^{(\text{sim})} - N_{\text{tot}}^{(\text{model})}) / \sigma_N]^2, \quad (10)$$

where y_i denotes $P_l(k)$ at each l and bin of k and \mathbf{p} include HOD parameters and the growth rate. The second term on the right-hand side represents the constraint on the total number of LRGs including both central and satellite LRGs. We give the error of N_{tot} as $\sigma_N = \sqrt{N_{\text{tot}}}$. The monopole and quadrupole spectra depend on the details of the 2-halo term, which depends on the details of cosmology and halo bias. We include the information of P_0 and P_2 upto $k = 0.2 h/\text{Mpc}$. On the other hand, high- l multipole such as

parameters	input	P_0, P_2	P_0, P_2, P_4	P_0, P_2, P_4, P_6
M_{\min}	5.7	5.28 ± 0.36	5.47 ± 0.23	5.45 ± 0.22
$\sigma_{\log M}$	0.7	0.66 ± 0.04	0.68 ± 0.02	0.68 ± 0.02
M_{cut}	3.5	6.2 ± 4.1	4.8 ± 2.4	4.4 ± 2.4
M_1	35	35 ± 13	34 ± 6	34 ± 5
α	1	0.96 ± 0.26	0.90 ± 0.21	0.94 ± 0.21

Table 1. HOD parameters in the functional form (eq.[8]) measured from different combinations of P_l for the simulated sample. The input values of HOD are also listed for reference. Covariance of P_l at different l and bins of k are included in the chi-square analysis. The mass is in unit of $10^{13} h^{-1} M_{\odot}$.

P_4 and P_6 mainly determined by the velocity distribution of satellite galaxies. To fully utilize the information, we include k upto $0.6h/\text{Mpc}$ for P_4 and P_6 .

Table 1 lists the best-fit values and the 1σ errors of the five HOD parameters in the functional form (eq.[8]). As seen in Figure 1, high- l multipole is sensitive to both the satellite fraction and the halo mass hosting satellites. It is found that the addition of the information of P_4 and P_6 reduces their error by nearly half. Upper panel of Figure 2 shows the reconstructed HOD from the different combinations of P_l of the simulated LRG samples when the functional form of HOD is assumed. The reconstructed HOD agrees with the input HOD (lines) within the 1-sigma error denoted by the shaded area. We also test if the input HOD can be reconstructed without assuming the functional form but fitting central and satellite HOD values at 5 different mass bins (10 HOD parameters in total). Lower panel of Figure 2 shows the comparison of fitted HOD values with the input HOD. We find that both central and satellite HODs are reproduced without need of the functional form.

4.3 Constraints on the growth rate

FoG is one of major systematic uncertainties in measuring the cosmic growth rate. High- l multipoles are sensitive to the satellite information and then help to break the degeneracy to improve the accuracy of growth rate measurement (Hikage & Yamamoto 2013). Table 2 shows the constraints on the satellite fraction and the velocity dispersion when using a functional form of HOD and direct fitting of HOD values at 5 different bins of mass. We find that addition of P_4 and P_6 improve the measurement of the growth rate by nearly twice (the error decreases from 8% to 4%) in both of the HOD parametrization.

Figure 3 shows the joint constraints on the fraction of satellite galaxies f_{sat} and the growth rate index γ , which is calculated with the simple approximation $f_z = \Omega_m^\gamma(z)$, and the satellite velocity dispersion $\sigma_v^{(\text{sat})}$ from different combinations of P_l . Satellite fraction and growth rate degenerate with each other because the suppression of quadrupole power due to satellite FoG effect is mimicked by increasing the growth rate f_z (or decreasing γ). Figure 3 shows that the addition of high- l multipole measurements breaks the degeneracy between f_{sat} and γ and then improves the accuracy of γ by nearly twice. The input values denoted by the cross symbols are successfully reproduced.

5 SUMMARY AND CONCLUSIONS

We present the analysis of HOD from multipole galaxy power spectra using the simulated catalogs which follows HOD of SDSS Lu-

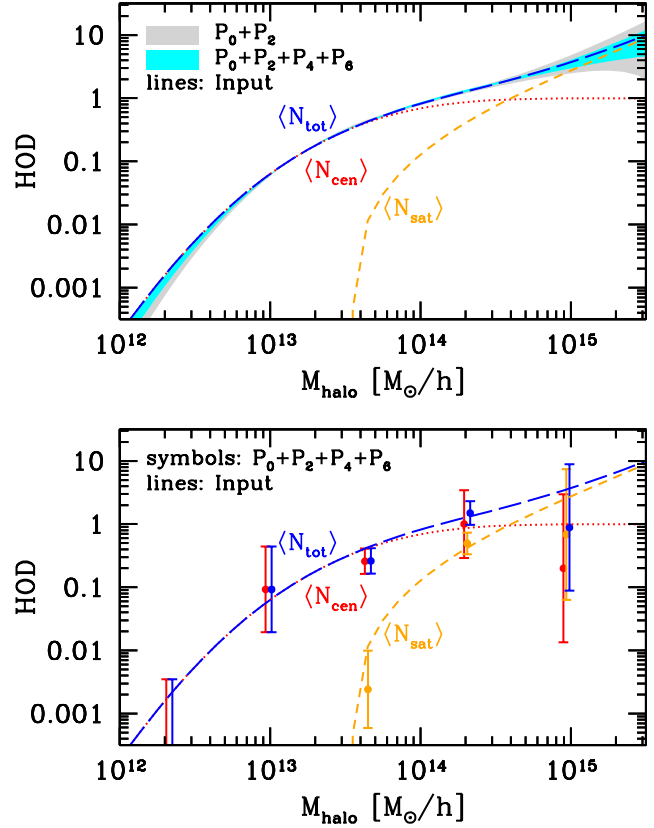


Figure 2. Reconstructed HOD by fitting HOD parameters to the multipole power spectra for the simulated LRG catalog. In upper panel, the functional form of HOD (eq. [8]) is assumed. Shaded area denote the $1\text{-}\sigma$ error of $\langle N_{\text{tot}} \rangle$ from P_0 and P_2 (Gray area) and P_0, P_2, P_4 and P_6 (light blue area). For reference, the input HOD for total (blue), central (red), and satellite galaxies (yellow) are plotted. In lower panel, central and satellite HOD values at 5 different mass bins are directly measured without assuming any functional form using P_0, P_2, P_4 and P_6 . The error-bars denote the $1\text{-}\sigma$ error.

parameters	input	P_0, P_2	P_0, P_2, P_4	P_0, P_2, P_4, P_6
HOD (eq. 8)				
$100f_{\text{sat}}$	6.5	5.8 ± 1.2	6.1 ± 0.7	6.2 ± 0.7
$\sigma_v^{(\text{sat})}$ [km/s]	570	590 ± 58	580 ± 29	576 ± 24
f_z/f_z^{GR}	1	1.01 ± 0.08	1.01 ± 0.05	1.02 ± 0.05
γ	0.55	0.55 ± 0.11	0.55 ± 0.07	0.54 ± 0.07
HOD (5 mass bins)				
$100f_{\text{sat}}$	6.5	30 ± 8	6.2 ± 1.1	6.2 ± 1.0
$\sigma_v^{(\text{sat})}$ [km/s]	570	270 ± 60	590 ± 40	565 ± 30
f_z/f_z^{GR}	1	1.03 ± 0.07	1.02 ± 0.05	1.02 ± 0.05
γ	0.55	0.53 ± 0.10	0.54 ± 0.06	0.54 ± 0.06

Table 2. Constraints on the satellite fraction f_{sat} , the satellite velocity dispersion $\sigma_v^{(\text{sat})}$, the growth rate normalized by the GR predictions f_z/f_z^{GR} and the growth rate index γ . The constraints comes from different combinations of P_l . We show the case when using a functional form of HOD in the equation 8 (Upper) and when fitting central and satellite HOD values at 5 different bins of halo mass as free parameters but assuming that $\langle N_{\text{sat}} \rangle$ increases as larger M (Lower).

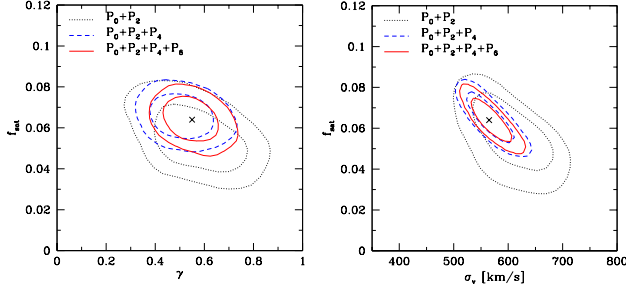


Figure 3. Joint constraints on the satellite fraction f_{sat} and the growth rate index γ (left) or $\sigma_v^{(\text{sat})}$ (right) from different combinations of multipole power spectra: $P_0 + P_2$ (red); $P_0 + P_2 + P_4$ (blue); $P_0 + P_2 + P_4 + P_6$ (black). Here we use a functional form of HOD (eq[8]). Each contour denotes 68% and 95% error respectively. The symbol of crosses denote the input values.

minous Red Galaxy. The high- l multipole power such as P_4 and P_6 are sensitive to the Fingers-of-God effect due to the large internal motion of satellite galaxies and thus they are useful probe to constrain the fraction and the velocity dispersion of satellite galaxies. We find that the HOD measurement is significantly improved by including high- l multipole spectra. We find that both central and satellite HOD can be reconstructed from P_l even without assuming any functional form of HOD.

FoG effect is a major uncertainty in constraining cosmic growth rate. High- l multipole information is useful for eliminating the uncertainty of the satellite FoG. Using simulated LRG catalogs, we find that the input value of satellite fraction/velocity dispersions and growth rate can be obtained from the multipole power spectra. We confirm that the addition of high- l multipole improve the accuracy of the growth rate measurement by nearly twice.

Our method is applicable for actual galaxy surveys such as SDSS and BOSS which mainly target LRGs. In this letter we simply use the $1(h^{-1}\text{Gpc})^3$ cubic box. For the actual observations, the leakage from the low- l multipole to high- l multipole due to the complicated survey geometry and radial selection function can be important (Beutler et al. 2013). The effect of the survey geometry and radial selection function can be evaluated by making the mock samples with the same geometry as the observation. Another observational issue is fiber collision, which makes difficult to measure the satellite fraction accurately. Various methods to correct the fiber collision effect has been developed (e.g., Guo et al. 2012). We also fix the cosmology and thereby fix the halo power spectra for simplicity. The uncertainty of cosmology mainly affect P_0 and P_2 in which the 2-halo term is dominant and then sensitive to the shape of the halo power spectra. On the other hand, high- l multipole power spectra are not sensitive to the details of the halo power spectrum because they are dominated by the 1-halo term. Even when fitting cosmology parameters together with HOD parameters, high- l multipole spectra should be still important to eliminate the satellite FoG effect. These works are beyond the scope of this letter and left for the future.

ACKNOWLEDGMENTS

We thank K. Yamamoto for useful discussions. The research is supported by Grant-in-Aid for Scientific researcher of Japanese

Ministry of Education, Culture, Sports, Science and Technology (No. 24740160).

REFERENCES

- Berlind A. A., Weinberg D. H., 2002, *ApJ*, 575, 587
 Berlind A. A. et al., 2003, *ApJ*, 593, 1
 Beutler F. et al., 2013, *ArXiv e-prints*
 Cooray A., Sheth R., 2002, *Physics Report*, 372, 1
 Crocce M., Pueblas S., Scoccimarro R., 2006, *MNRAS*, 373, 369
 Duffy A. R., Schaye J., Kay S. T., Dalla Vecchia C., 2008, *MNRAS*, 390, L64
 Eisenstein D. J. et al., 2001, *AJ*, 122, 2267
 Geach J. E., Sobral D., Hickox R. C., Wake D. A., Smail I., Best P. N., Baugh C. M., Stott J. P., 2012, *MNRAS*, 426, 679
 George M. R. et al., 2012, *ApJ*, 757, 2
 Guo H., Zehavi I., Zheng Z., 2012, *ApJ*, 756, 127
 Guzzo L., et al., 2008, *Nature*, 451, 541
 Hikage C., Mandelbaum R., Takada M., Spergel D. N., 2013, *MNRAS*, 435, 2345
 Hikage C., Takada M., Spergel D. N., 2012, *MNRAS*, 419, 3457
 Hikage C., Yamamoto K., 2013, *JCAP*, 8, 19
 Jackson J. C., 1972, *MNRAS*, 156, 1P
 Kravtsov A. V., Berlind A. A., Wechsler R. H., Klypin A. A., Gottlöber S., Allgood B., Primack J. R., 2004, *ApJ*, 609, 35
 Lewis A., Challinor A., Lasenby A., 2000, *ApJ*, 538, 473
 Mandelbaum R., Seljak U., Kauffmann G., Hirata C. M., Brinkmann J., 2006, *MNRAS*, 368, 715
 Masaki S., Lin Y.-T., Yoshida N., 2013, *MNRAS*, 436, 2286
 Masjedi M. et al., 2006, *ApJ*, 644, 54
 Navarro J. F., Frenk C. S., White S. D. M., 1997, *ApJ*, 490, 493
 Nishimichi T., Oka A., 2013, *ArXiv e-prints*
 Oka A., Saito S., Nishimichi T., Taruya A., Yamamoto K., 2013, *ArXiv e-prints*
 Okumura T., Matsubara T., Eisenstein D. J., Kayo I., Hikage C., Szalay A. S., Schneider D. P., 2008, *ApJ*, 676, 889
 Peacock J. A., et al., 2001, *Nature*, 410, 169
 Reid B. A. et al., 2012, *MNRAS*, 426, 2719
 Reid B. A., Spergel D. N., 2009, *ApJ*, 698, 143
 Samushia L. et al., 2013, *ArXiv e-prints*
 Sato T., Hütsi G., Yamamoto K., 2011, *Progress of Theoretical Physics*, 125, 187
 Seljak U., 2000, *MNRAS*, 318, 203
 Skibba R. A., van den Bosch F. C., Yang X., More S., Mo H., Fontanot F., 2011, *MNRAS*, 410, 417
 Springel V., 2005, *MNRAS*, 364, 1105
 White M., 2001, *MNRAS*, 321, 1
 White M. et al., 2011, *ApJ*, 728, 126
 Yamamoto K., Nakamura G., Hütsi G., Narikawa T., Sato T., 2010, *Phys. Rev. D*, 81, 103517
 Yamamoto K., Sato T., Hütsi G., 2008, *Progress of Theoretical Physics*, 120, 609
 Zehavi I. et al., 2005, *ApJ*, 630, 1
 Zheng Z., Zehavi I., Eisenstein D. J., Weinberg D. H., Jing Y. P., 2009, *ApJ*, 707, 554
 Zheng Z., et al., 2005, *ApJ*, 633, 791